

1 Efficiency of attack strategies on complex model and real-world networks

2

3 Michele Bellingeri^{1*}, Davide Cassi¹, Simone Vincenzi^{2,3}

4

5 ¹Dipartimento di Fisica, Università di Parma, via G.P. Usberti, 7/a, 43124 Parma, Italy

6 ²Center for Stock Assessment Research (CSTAR) and Department of Applied Mathematics
7 and Statistics, University of California Santa Cruz, 110 Shaffer Road, 95060 Santa Cruz,
8 CA, US.

9 ³Dipartimento di Elettronica, Informazione e Bioingegneria, Politecnico di Milano, Via
10 Ponzio 34/5, I-20133 Milan, Italy

11 * Corresponding author: michele.bellingeri@nemo.unipr.it

12

13 Abstract

14 We investigated the efficiency of attack strategies to network nodes when targeting several
15 complex model and real-world networks. We tested 5 attack strategies, 3 of which were
16 introduced in this work for the first time, to attack 3 model (Erdos and Renyi, Barabasi and
17 Albert preferential attachment network, and scale-free network configuration models) and
18 3 real networks (Gnutella peer-to-peer network, email network of the University of Rovira
19 i Virgili, and immunoglobulin interaction network). Nodes were removed sequentially
20 according to the importance criterion defined by the attack strategy. We used the size of
21 the largest connected component (*LCC*) as a measure of network damage. We found that
22 the efficiency of attack strategies (fraction of nodes to be deleted for a given reduction of
23 *LCC* size) depends on the topology of the network, although attacks based on the number
24 of connections of a node and betweenness centrality were often the most efficient
25 strategies. Sequential deletion of nodes in decreasing order of betweenness centrality was
26 the most efficient attack strategy when targeting real-world networks. In particular for
27 networks with power-law degree distribution, we observed that most efficient strategy
28 change during the sequential removal of nodes.

29

30 1. Introduction

31 The resilience of real-world complex networks, such as Internet, electrical power grids,
32 airline routes, ecological and biological networks [1,2,3,4,5,6] to “node failure” (i.e. node
33 malfunctioning or removal) is a topic of fundamental importance for both theoretical and
34 applied network science. Node failure can cause the fragmentation of the network, which
35 has consequences in terms of system performance, properties, and architecture, such as
36 transportation properties, information delivery efficiency and the reachability of network
37 components (i.e. ability to go from node of the network to another) [3].

38 Several studies [3,7,8,9] have investigated the resilience of model networks using a
39 number of “attack strategies”, i.e. a sequence of node removal according to certain
40 properties of the nodes [2,3,7]. A widely-applied attack strategy consists in first ranking
41 the nodes with respect to an importance criterion (e.g. number of connections or some
42 measures of centrality) and then remove the nodes sequentially from the most to the least
43 important according to the chosen criterion until the network either becomes disconnected
44 or loses some essential qualities [3,10]. However, little is known on how the efficiency (i.e.
45 fraction of nodes to be deleted for a given change in the network) of attack strategies
46 varies when considering differing real-world and model networks.

47 In addition, an interesting - although underappreciated - issue is how the relative
48 efficiency of attack strategies may change during the attack. For example, an attack
49 strategy might be more efficient when the targeted (i.e. under attack) network is still
50 pristine, while other strategies might be more efficient when the network has already been
51 fragmented and some of its properties been compromised. Testing the efficiency of the
52 different attack strategies when targeting different networks may also allow to identify the

53 most important nodes for network functioning, and therefore which nodes should be
54 primarily protected, as in the case of computer [11] or ecological networks [6,12,13,14], or
55 removed, as in the case of immunization/ disease networks [15].

56 In this work, we test the efficiency of both well-known attack strategies and new strategies
57 introduced for the first time in this paper when targeting either model or real-world
58 networks, using the size of the largest connected component (*LCC*) (i.e. the largest number
59 of nodes connected among them in the network, [2]) as a measure of network damage. We
60 found for model networks that the best strategy to reduce the size of the *LCC* depended on
61 the topology of the network that is attacked. For real-world networks, the removal of
62 nodes using betweenness centrality as importance criterion was consistently the most
63 efficient attack strategy. In addition, we found that for some networks an attack strategy
64 can be more efficient than others up to a certain fraction of nodes removed, but other
65 attack strategies can become more efficient after that fraction of nodes has been removed.

66 2.Methods

67 2.1 Attack strategies

68 We attacked the networks by sequentially removing nodes following some importance
69 criteria. We compared the efficiency of a pool of attacks strategies, some of which have
70 been already described in the literature while others are introduced in this work for the
71 first time. Most of the analyses on the robustness of network when have investigated the
72 effect of removing nodes according to their rank (i.e. number of links) or some measures of
73 centrality [3,10,16]. In this work, we introduce new attack strategies that focus entirely or
74 in part on less local properties of a node, in particular its number of second neighbors, as
75 explained in detail below.

76 Several indexes and measures have been introduced to describe network damage. In this
77 work, we use the size of the largest connected component (*LCC*), i.e. the size of the largest
78 connected sub-graph in the network [2,3], as a measure of network damage during the
79 attack. A faster decrease in the size of the *LCC* indicates a more efficient attack strategy. In
80 order to compare attack strategies across networks, we used the normalized *LCC* size with
81 respect to the starting *LCC* size, i.e. the number of nodes in the *LCC* before any removal.

82 For each attack strategy, we applied both the recalculated and non-recalculated methods.
83 In the recalculated method, the property of the node relevant for the attack strategy (e.g.
84 number of links) was recalculated after each node removal. In the non-recalculated
85 method, the property of the node was computed before the first node removal and was
86 not updated during the sequential deletion of nodes. An attack strategy is less efficient
87 than another when a higher the fraction of nodes has to be removed to reduce the *LCC* to
88 zero (or any other size). With q we indicate the fraction of nodes removed during the
89 sequential removal of nodes.

90 We used 2 attack strategies that have been already described in the literature. *First-degree*
91 *neighbors (First)*: nodes are sequentially removed according to the number of first
92 neighbors of each node (i.e. node rank). In the case of ties (i.e. nodes with the same rank),
93 the sequence of removal of nodes is randomly chosen. *Nodes betweenness centrality (Bet)*:
94 nodes are sequentially removed according to their betweenness centrality, which is the
95 number of shortest paths from all vertices to all others that pass through that node [3,17].

96 We introduced in this paper the following new attack strategies. *Second-degree neighbors*
97 *(Sec)*: nodes are sequentially removed according to the number of second neighbors of
98 each node. Second neighbors of node j are nodes that have a node in common with, but

99 are not directly connected to, node j . *First + Second neighbors (F+S)*: nodes are deleted
100 according to the sum of first and second neighbors of each node. *Combined first and second*
101 *degree (Comb)*: nodes are removed according to their rank. In the case of ties, nodes are
102 removed according to their second degree.

103 For all attack nodes were sequentially removed from most to least connected, or in case of
104 *Bet*, from higher to lower betweenness centrality.

105 2.2 Networks

106 We tested the attack strategies described in Section 2.2 on (i) 3 types of model networks
107 and (ii) 3 real world networks.

108 The networks we used are undirected and unweighted graphs in which nodes are
109 connected by links or edges, and rank k of a node is the number of links of that node. Each
110 link may represent several real world interactions. For instance, in social networks links
111 between nodes represent interactions between individuals or groups, such as
112 co-authorship in scientific publications or friendship [2]. In cellular networks, nodes are
113 chemicals species connected by chemical reactions [18], while in ecological networks links
114 describe the trophic interactions between species or group of species, e.g. the energy and
115 matter passing from prey to predator [6,14,19,20].

116 2.2.1 Model networks

117 We tested the attack strategies on (i) Erdos and Renyi graphs [21], (ii) Barabasi and Albert
118 preferential attachment networks [2], and (iii) scale-free network configuration models
119 [22]. For each model network, we tested models of different size, as explained below. Since
120 each model network is a random realization of the network-generating mechanism, we

121 tested the attack strategies on 50 random realizations of each model network used the
122 mean of the normalized LCC size at each fraction q of nodes removed as a measure of
123 network damage. We observed a small variation of LCC size at each fraction q of nodes
124 removed across different realizations of networks, thus the mean LCC size across
125 replicates well represents the overall behavior of the attack strategy.

126 The Erdos and Renyi (ER) model generates a random graph with N nodes connected by L
127 links, which are chosen randomly with an occupation probability p from $L_{\max} = N(N-1)/2$
128 possible links, i.e. p is the proportion of realized links from L_{\max} . The expected number of
129 links is $\langle L \rangle = (N^2 p)/2$ and the expected rank of a node is $\langle k \rangle = Np$. The random graph can
130 be defined by the number of nodes N and the probability p , i.e. $ER(N,p)$ [21]. We analyzed
131 ER graphs with different values of N and p , namely: $ER(N = 500, p = 0.008)$, $ER(1\ 000,$
132 $0.004)$, $ER(10\ 000, 0.0004)$.

133 The Barabasi and Albert preferential attachment network (BA) is created starting from few
134 isolated nodes and then growing the network by adding new nodes and links [2]. At each
135 step in the creation of the network, one node and m outgoing links from the new node are
136 added to the network. The probability θ that the new node will be connected to node i

137 already in the network is function of the degree k_i of node i , such that $\theta(k_i) = k_i / \sum_{j=N}^{j=1} k_j$ (i.e.

138 preferential attachment, since more connected nodes are more likely to be connected to the
139 new node) [2]. The BA network is defined by parameters N and m , i.e. $BA(N,m)$. We built
140 BA scale free networks with parameters $BA(N=500, m = 2)$, $BA(1\ 000, 2)$, $BA(10\ 000, 2)$.

141 We created networks with power-law degree distribution using the configuration model
142 for generalized random graphs [2,22,]. This model is defined as follows. A discrete degree

143 distribution $P(K = k) = k^{-\alpha}$ is defined, such that $P(k)$ is the proportion of nodes in the
144 network having degree k . The maximum node degree k_{\max} is equal to N , where N is the
145 number of nodes. The domain of the discrete function $P(k)$ becomes $(1, k_{\max})$. We generated
146 the degree sequence of the nodes by randomly drawing N values k_1, \dots, k_n from the degree
147 distribution. Then, for each node i we drew a link with node j with probability $P(k_i)P(k_j)$. A
148 scale free configuration model network is defined by parameters N, α and $\langle k \rangle$. We
149 analyzed scale free network with parameters $CM(N = 500, \alpha = 2.5, \langle k \rangle = 3.8)$, $CM(1$
150 $000, 2.5, 3.8)$, $CM(10\ 000, 2.5, 3.9)$.

151 2.2.2 Real world networks

152 We tested the attack strategies on the following real-world networks: (i) The Gnutella P2P
153 (peer-to-peer) network (*Gnutella*) [24], (ii) the email network of the University Rovira i
154 Virgili (URV) in Tarragona, Spain (*Email*) [25], and (iii) the immunoglobulin interaction
155 network (*Immuno*) [26]. Nodes of *Gnutella* ($N=8846, L=31839$) represent hosts in the peer-
156 to-peer network while links represent connections between the hosts [24]. *E-mail* ($N=1134,$
157 $L=10902$) provides a representative example of the flow of information within a human
158 organization [25]. *Immuno* is the undirected and connected graph of interactions in the
159 immunoglobulin protein ($N = 1316, L = 6300$) where nodes represent amino acids and two
160 amino acids are linked if they interact in the immunoglobulin protein [26].

161 3. Results

162 3.1 Non-Recalculated method

163 3.1.1 Model networks (Fig. 1)

164 **ER:** For all sizes of networks, the 5 attack strategies were equally efficient in reducing the
165 size of the *LCC* up to $q \approx 0.2$. For $q > 0.2$, *First* was the most efficient strategy to reduce the
166 size of the *LCC*.

167 **CM:** For $N = 500$, *Comb* was the most efficient strategy early in the removal sequence.,
168 while *First* became the most efficient strategy after $q > 0.1$. For $N = 1\,000$, *Comb*, *Bet*, and
169 *First* had the same efficiency. For $N = 10\,000$, *Comb*, *Bet*, and *First* were equally efficient up
170 to $q = 0.1$, while for $q > 0.1$ *First* was the most efficient strategy.

171 **BA:** For $N = 500$, *First*, *Comb* and *Bet* were equally efficient in reducing the size of the *LCC*.
172 For bigger networks, *First*, *Comb* and *Bet* were equally efficient up to $q = 0.8$ ($N = 1\,000$)
173 and $q = 0.5$ ($N = 10\,000$). Then, *Bet* became more efficient than *First* and *Comb*.

174 3.1.2 Real-world networks (Fig. 2)

175 **Email:** *Bet* was the most efficient strategy to reduce *LCC* up to $q \approx 0.3$. For greater
176 fractions of nodes removed, *First* and *Comb* were slightly more efficient than *Bet*.

177 **Immuno:** *Bet* was distinctly more efficient than other strategies up to $q = 0.55$. For $q > 0.55$,
178 all strategies were equally efficient.

179 **Gnutella:** *Bet* was the most efficient attack strategy.

180 3.2 Recalculated

181 3.2.1 Model networks (Fig. 3)

182 **ER:** *First* and *Comb* were the most efficient strategies to reduce the *LCC* up to $q \approx 0.2$.

183 Beyond that fraction of nodes removed, *Bet* became more efficient than *First*. *Sec* was the
184 least efficient strategy.

185 **CM:** *Comb* was the most efficient strategy up to $q \sim 0.1$. Beyond that, *Bet* was the most
186 efficient strategy, while *Sec* was the least efficient strategies.

187 **BA:** *Comb* was the most efficient strategy up to $q \sim 0.1$. First, *F+S* and *Bet* attack induced a
188 slightly slower decrease in *LCC* size. When q reached 0.1, *Bet* became the most efficient
189 strategy. *Sec* was the least efficient strategy.

190 3.2.2 Real-world networks (Fig. 4)

191 **Email:** All attack strategies were equally efficient up to $q = 0.12$. For $q > 0.12$ *Bet* was the
192 most efficient attack strategy.

193 **Immuno:** *Bet* was largely the most efficient attack strategy.

194 **Gnutella:** All attack strategies were equally efficient up to $q = 0.1$. For $q > 0.1$ *Bet* was the
195 most efficient attack strategy.

196 4. Discussion

197 We discuss the following main results of our work: (i) attacks were largely more efficient
198 (i.e. smaller fraction of nodes deleted to achieve the same reduction in *LCC* size) with the
199 recalculated than with the non-recalculated method; (ii) the efficiency of attack strategies
200 on model networks depended on network topology; (iii) the sequential removal of nodes
201 according to their betweenness centrality was the most efficient attack to real-world
202 networks; (iv) for some networks, the relative efficiency of attack strategies changed
203 during the removal sequence.

204 We found that the recalculated method provided more efficient attacks than the non-
205 recalculated method, i.e. for a given fraction of nodes removed a larger reduction of *LCC*

206 was obtained with the recalculated method. This result confirms the findings of other
207 analyses on robustness of networks [2,3], which found that updated information on the
208 topology of the system after each removal allowed for more efficient attacks to networks.
209 However, non-recalculated attack strategies are implemented in various relevant settings
210 and are equivalent in practice to the simultaneous removal of nodes, as it happens in the
211 case of vaccination campaigns (i.e. vaccinating at the same time nodes of the contact
212 network with the highest probability of acquiring or transmitting the disease) or attacks to
213 computer networks [11].

214 For model networks, the efficiency of the attack strategies depended on network topology.
215 In the case of networks with power-law degree distribution, the efficiency of the attack
216 strategies depended also on network size. Across all model networks and considering both
217 the non-recalculated and recalculated methods, attack strategies based on either the
218 betweenness centrality of nodes or node rank were the most efficient ones. However, the
219 sequential deletion of nodes according to their betweenness centrality was consistently the
220 most efficient attack strategy to real-world networks, with the only exception of the attack
221 to the *Email* network with the non-recalculated method. While in some cases *Bet* was
222 slightly more efficient than other strategies in reducing the size of the largest connected
223 component, in others *Bet* was largely the most efficient strategy. For example, in the
224 immunoglobulin interaction network, deleting a very small fraction of nodes with high
225 betweenness centrality reduced the size of the normalized *LCC* of more than 60% using
226 either the recalculated and non-recalculated method, while for the same fractions of nodes
227 removed other attack strategies were able to obtain only a 1-5% reduction in *LCC* size.
228 Betweenness centrality describes how “central” a node is in the network by considering

229 the fraction of shortest paths that pass through that node [17]. Nodes with betweenness
230 centrality greater than 0 play a major role in connecting areas of the network that would
231 otherwise be either sparsely connected or disconnected [23]. This makes betweenness
232 centrality an important centrality measure for a social, technological, computer, and
233 biological networks. The higher efficiency of the strategy based on node betweenness
234 centrality with respect to the attack based on node rank in real-world networks can be
235 explained by the fact that in real-world networks some of the critical nodes (i.e. nodes
236 whose persistence strongly contribute to maintaining network integrity) are either not
237 highly linked, or that the highly linked nodes are not located in the network core [23].

238 The newly-introduced *Combined* attack strategy, when recalculated, was the most efficient
239 strategy to decrease *LCC* size in the scale free network configuration model and in the
240 Barabasi-Albert model up to $q = 0.1$, performing slightly better than the attack based on
241 node rank (*First* strategy). The *Combined* attack first select nodes according to their rank,
242 then, in the case of ties (i.e. nodes with the same rank), it sequentially removes nodes
243 according to their second degree. On the contrary, in the case of ties *First* randomly
244 chooses the removal sequence for the nodes with the same rank. Thus, at the beginning of
245 the attack to the network, when two or more major hubs have the same number of links to
246 other nodes, selecting to remove first the hub with the greatest second degree causes a
247 faster decrease in *LCC* size than to randomly select the removal sequence for those hubs.

248 Later in the attack, the *Combined* strategy was less efficient than the *First* strategy to attack
249 scale free networks; this might be due to the fact that after a certain fraction of hubs has
250 been deleted, removing first (in the case of ties) the node(s) with the highest second

251 degree(s) would remove more peripheral and less important nodes. Those nodes are less
252 likely to be part of the largest connected component.

253 Lastly, the efficiency of attack strategies changed along the sequential removal of nodes.
254 This was particularly evident for networks with power-law degree distribution. It follows
255 that the percolation threshold, i.e. the fraction of nodes removed for which the size of the
256 largest connected component reaches zero, might be for some networks little correlated
257 with the fraction of nodes to be removed in order to reduce the largest connected
258 component to a size greater than 0. This result has important implications for applied
259 network science and deserves further investigations. For example, in the case of
260 immunization strategies, choosing the attack strategy according to the percolation
261 threshold may be of little use when the goal is to reduce as much as possible the size of
262 *LCC* with just a few targeted immunizations.

263

264 Acknowledgements

265 We thank Riccardo Campari, Daniele Marmiroli and Prof. Alessio Camobreco for useful
266 comments on a previous version of the manuscript.

267

268 References

- 269 [1] D. S. Callaway, M. E. Newman, S. H. Strogatz, and D. J. Watts, Phys. Rev. Lett. **85**, 5468
270 (2000).
- 271 [2] R. Albert and A. Barabási, Rev. Mod. Phys. **74**, (2002).
- 272 [3] P. Holme, B. J. Kim, C. N. Yoon, and S. K. Han, Phys. Rev. E **65**, 056109 (2002).

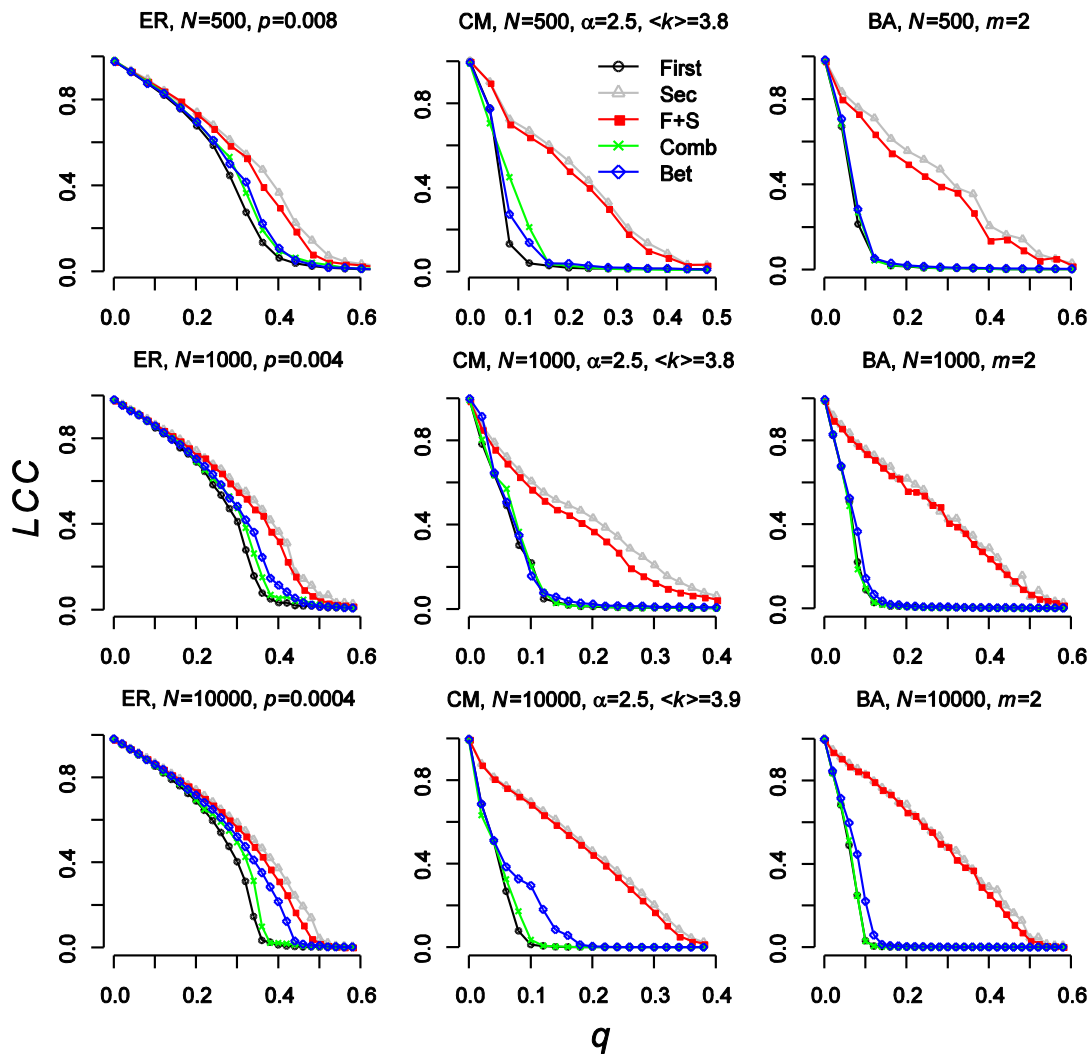
- 273 [4] A. Bodini, M. Bellingeri, S. Allesina, and C. Bondavalli, *Philos. Trans. R. Soc. Lond. B.*
274 *Biol. Sci.* **364**, 1725 (2009).
- 275 [5] E. Agliari, A. Barra, S. Bartolucci, A. Galluzzi, F. Guerra, and F. Moauro, *Phys. Rev. E* **87**,
276 042701 (2013).
- 277 [6] M. Bellingeri, D. Cassi, and S. Vincenzi, *Ecol. Model.* **251**, 1 (2013).
- 278 [7] P. Crucitti, V. Latora, M. Marchiori, and A. Rapisarda, *Phys. A Stat. Mech. Its Appl.* **340**,
279 388 (2004).
- 280 [8] J. Ø. H. Bakke, A. Hansen, and J. Kertész, *Europhys. Lett.* **76**, 717 (2006).
- 281 [9] G. Dong, J. Gao, R. Du, L. Tian, H. E. Stanley, and S. Havlin, *Phys. Rev. E* **87**, 052804
282 (2013).
- 283 [10] R. Albert, H. Jeong, and A. Barabasi, *Nature* **406**, 378 (2000).
- 284 [11] R. Cohen, K. Erez, D. ben-Avraham, and S. Havlin, *Phys. Rev. Lett.* **86**, 3682 (2001).
- 285 [12] R. V Solé and J. M. Montoya, *Proc. Biol. Sci.* **268**, 2039 (2001).
- 286 [13] A. Curtsdotter, A. Binzer, U. Brose, F. de Castro, B. Ebenman, A. Eklöf, J. O. Riede, A.
287 Thierry, and B. C. Rall, *Basic Appl. Ecol.* **12**, 571 (2011).
- 288 [14] B. Ebenman, *J. Anim. Ecol.* **80**, 307 (2011).
- 289 [15] R. Pastor-Satorras and A. Vespignani, *Phys. Rev. E* **65**, 036104 (2002).
- 290 [16] L. K. Gallos, R. Cohen, P. Argyrakis, A. Bunde, and S. Havlin, *Phys. Rev. Lett.* **94**, 188701
291 (2005).
- 292 [17] M. Barthélemy, *Eur. Phys. J. B* **38**, 163 (2004).
- 293 [18] H.-W. Ma and a.-P. Zeng, *Bioinformatics* **19**, 1423 (2003).
- 294 [19] J. a. Dunne, R. J. Williams, and N. D. Martinez, *Ecol. Lett.* **5**, 558 (2002).
- 295 [20] M. Bellingeri and A. Bodini, *Theor. Ecol.* **6**, 143 (2012).
- 296 [21] P. Erdos and A. Renyi, *Publ. Math. Inst. Hung. Acad. Sci.* **5**, 17 (1960).
- 297 [22] S. Dorogovtsev, a. Goltsev, and J. Mendes, *Rev. Mod. Phys.* **80**, 1275 (2008).
- 298 [23] M. E. J. Newman, *SIAM Rev.* **45**, 167 (2003).
- 299 [24] M. Ripeanu, I. Foster., and A. Iamnitch, *IEEE Internet Comput. Journal* **6**, 50 (2002).
- 300 [25] R. Guimera, L. Danon, A. Diaz-Guilera, F. Giralt, A. Arenas, *Phys Rev E* **68**, 065103 (2003)

301 [26] D. Gfeller, PhD Thesis EPFL, (2007)

302

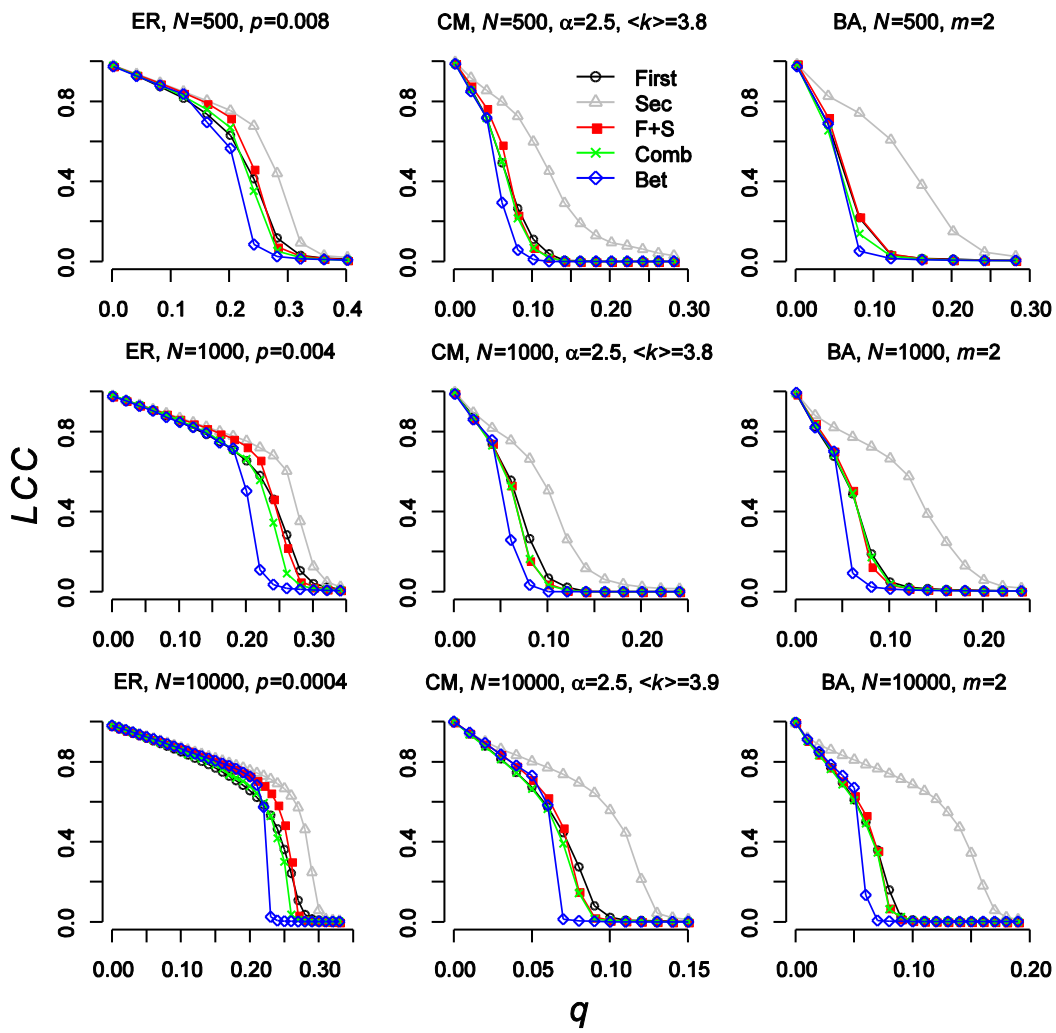
303

304



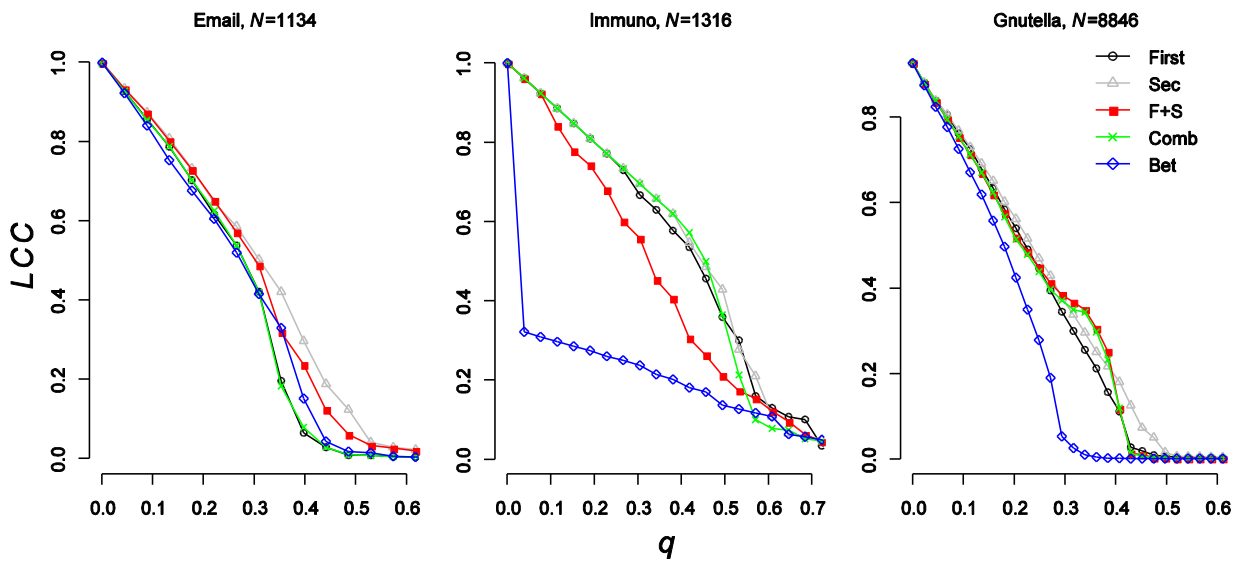
306

307 **Figure 1.** Size of normalized LCC and the fraction q of nodes removed for non-recalculated
 308 targeted attacks to model networks. Points are plotted every 20 nodes removed for networks with N
 309 = 500 and $N=1\ 000$, and every 200 nodes removed for $N=10000$.



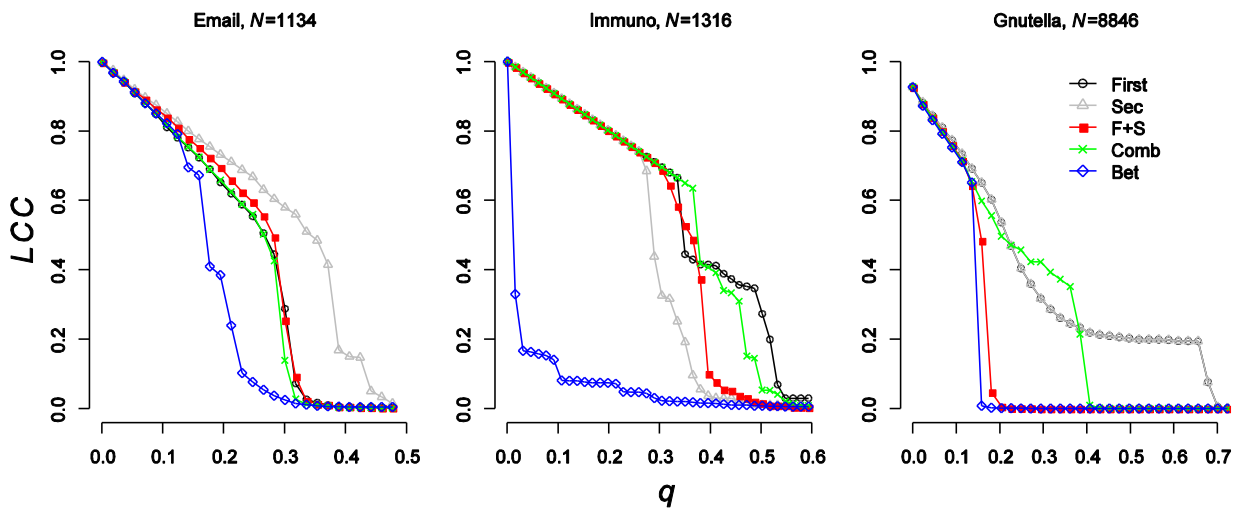
310

311 **Figure 2.** Size of normalized LCC and the fraction q of nodes removed for non-recalculated
 312 targeted attacks to real-world networks. Points are plotted every 50 nodes removed for *Email* and
 313 *Immuno* networks, and every 200 nodes removed for *Gnutella*.



314

315 **Figure 3.** Size of normalized LCC and the fraction q of nodes removed for recalculated targeted
 316 attacks to model networks. Points are plotted every 20 nodes removed for networks with $N = 500$
 317 and $N = 1\,000$, and every 200 nodes removed for $N = 10\,000$.



318

319 **Figure 4.** Size of normalized LCC and the fraction q of nodes removed for recalculated targeted
 320 attacks to real-world networks. Points are plotted every 50 nodes removed for *Email* and *Immuno*
 321 networks, and every 200 nodes removed for *Gnutella*.

322